applied sciences

MDPI

Article

Study of Heat Distribution in Railway Switch Using Resistive Heater in Cold Climate Conditions

Arefeh Lotfi *, Adeel Yousuf and Muhammad Shakeel Virk

Arctic Technology & Icing Research Group, UiT–The Arctic University of Norway, 8514 Narvik, Norway; yousuf.adeel@uit.no (A.Y.); muhammad.s.virk@uit.no (M.S.V.)
* Correspondence: arefeh.lotfi@uit.no

Abstract: The railway is an essential source of logistics and transportation in cold regions, but low temperatures and icing can be challenging for uninterrupted railway operations in these regions. Icing on railway switches is a safety hazard, and presently, one of the industry's adaptive approaches for ice mitigation is the use of resistive heaters. This method is efficient but consumes a great amount of electricity, leading to high financial costs in terms of the operation and maintenance of railway tracks in ice-prone regions. In this paper, a study is carried out using experiments and computational simulations to analyze the heat distribution in a cross-section of a rail at below-freezing temperatures. Experiments are performed in a cold room using an actual rail switch, thermocouples, and infrared imaging, while numerical analyses are carried out using a MATLAB-based analytical model to simulate the heat transfer, considering a section of stock rail and a heating element. Results show a considerable loss of heat from the heater to the surroundings of the rail, especially towards the ground ballast. Numerical simulation results provide a good insight into heat transfer along railway sections, and results are validated with experiments, where a good agreement is found. This study provides a good base for further optimization of resistive heating operations for ice mitigation along railway switches.

Keywords: icing; railway switch; cold room; thermocouples; analytical model; infrared

Citation: Lotfi, A.; Yousuf, A.; Virk, M.S. Study of Heat Distribution in Railway Switch Using Resistive Heater in Cold Climate Conditions. *Appl. Sci.* **2024**, *14*, 8151. https://doi.org/10.3390/app14188151

Academic Editor: Demis Pandelidis

Received: 7 July 2024
Revised: 31 July 2024
Accepted: 6 September 2024
Published: 11 September 2024

1. Introduction

The parts of railroad tracks that allow trains to switch between tracks are known as railway switches, turnouts, or points. Based on their operational performance and safety, switches play a critical role in the network. However, ice and snow accumulation on these switches can impede their movement, leading to operational issues and safety concerns. To avoid these problems, the railway industry is using a variety of anti-icing and de-icing techniques. These methods include hot air blowers, chemicals, gas heating, water, and geothermal heating. Among railway switch heating methods, resistive electrical heaters are more common, especially in Europe [1–6]. Such electrical heaters produce heat when the current passes through a resistive material. The primary component is a flat or oval-shaped resistive heater installed on the stock rail foot (Figure 1). The optimal location of the heater on the rail and the need for extra special equipment can vary depending on the kind of turnout and the environment [6].

Despite its simple design and ease of installation, resistive electrical heaters do not have high electrical and thermal efficiency. These heaters heat the entire rail and use significant electrical energy for the lengthy rail. Also, the heat radiates faster from the rail since it is larger than the heater and has a high volume in contact with the air temperature differential [7]. Over the years, it has been observed that resistive electrical systems are not capable of heating turnouts efficiently. Researchers have examined several design approaches for resistive heater performance improvement. Design changes have been made to the resistive heaters, which include: (1) expanding the contact area between

the heater and rail by converting the heating element's shape from cylindrical to flat; (2) modifying the outer sheath material of the heating element to make it resistant to most chemicals, water, and salt; (3) converting the embedded resistance wire's linear shape to a helical one; (4) utilization of insulating material to conceal the heating element on the air-facing surface [8]; and minimizing hot air loss by using covers, which can reduce energy costs and protect switches from harsh weather [9].

Figure 1. Railway switch operation in icing conditions and location of heater [2].

Induction heating for railway switches was first introduced and tested in Poland in the year 1978 for some selected switches. In this design, rails were heated with eddy currents induced inside the rails. Heating wires were insulated and were not in contact with the rails in a galvanic way. Through the years, this method has evolved, and researchers have performed several studies on this concept. In 2012, Szychta et al. reviewed this concept and developed a 3D simulation model. In this study, they analyzed the electric and magnetic characteristics of rails in the presence of induction heating using the Flux3D [1]. In 2021, another study was published, where researchers compared the melting time of an ice cube, the temperature of the rail, and energy consumption between induction heating at different frequencies and conductive heaters. The results showed that the induction system sends the heat to ice and snow directly, while in the conductive heater, a great amount of heat is stored in the stock rail, which increases the energy consumption of this method. Results did not show that induction heating was an absolutely better method than the conduction system. In some frequencies, it performed better in the melting time and energy consumption, so it is possible to find the optimal situation for induction heating, which can save up to 70% of energy compared to the resistive method [6].

In 2015, Flis conducted a numerical study to compare resistive and inductive heating systems of railway switches. He simulated heat transfer and calculated respective heat losses. In this study, he did not consider phase transformation and melting. The results showed that a huge amount of thermal energy was absorbed by the rail due to its high heat capacity, and a considerable amount of heat was radiated into the air. He claimed that the induction plate reached the final temperature in only 4 min, and then the melting started, while for resistive heating, this process took two hours. Also, it was mentioned that the ice area (workplace) received more heat energy from induction heating rather than resistive heating [10].

In another comparison study between resistive heating and induction heating, researchers conducted experiments in a climate chamber on a railway switch at different environmental temperatures and various distances between stock and switch rails. Results showed higher energy efficiency of induction heating than resistive heating, as in the induction system, the heat transferred directly from the heating plate to the purpose area. Moreover, induction heating also improved the lubrication circumstances of moving turnout components [11].

Contactless heaters have also been suggested for railways since the stock rail loses a lot of energy due to its high heat absorption capacity. Flis [12] performed a study on contactless heater performance in 2018 using experiments and numerical simulations. He compared the energy efficiency and heat distribution in the railway turnout. Results showed that for a constant time of heating, the temperature of the contactless system area was higher than the classic one; also in this situation, the snow area received more heat

from the contactless area rather than the classic one [12]. In 2020, Flis continued his work and explained that it is necessary to optimize the current heating system. He examined two modifications to the conventional heating system. The study showed that the existing heating method's performance is suboptimal and that the contactless approach is more effective. However, he recommended that the heater element's ideal shape needs to be optimized [13]. In 2019, researchers from Korea conducted a study on using high-frequency induction to heat railroad switches. They designed and analyzed an electronic circuit to control the high-frequency induction heating system. Also, the eddy current functioning as a heat source was observed using electromagnetic analysis [14]. The results of this study showed that the temperature of the induction heater can increase in a shorter time than that of the resistive method.

According to the literature and interviews with industry experts, it seems that the resistive heating method is a costly operation due to high electricity consumption. Some work has been done to introduce new methods of heating or improve the performance of the current method, but still, these suggestions are in the lab testing of the prototype phase. Also, as conductive electrical heaters are operated on a large scale, replacement of this method is difficult due to the high infrastructure cost involved. The study in this paper aims to provide a scientific basis for optimizing the resistive heating operations for ice mitigation along railway switches. Both experimental and numerical methods are used. Investigation of the heat distribution in railway switches is expected to identify an optimal approach to reducing the operation cost of conductive electrical heaters.

2. Materials and Methods

This study was carried out using lab-based experiments and numerical simulations. Experiments were carried out in a cold room chamber facility at UiT, whereas, for numerical simulations, a MATLAB-based analytical model of heat transfer was developed. For lab-based experiments, the setup was developed using the actual railway switches obtained from the railway department. The setup was developed in the cold room facility where the temperature could be controlled up to 248 K (−25 °C). A reactive electrical heater was used for heating. This heater contained wire and element parts. The element part was attached to the rail using four clamps. These clamps were specified for the rail and heater type. Ballasts and soil were provided under the rails to make the conditions as real as possible. Temperature was recorded using thermocouples and infrared cameras. Various thermocouples were attached along the 2 m long rail track, and data were recorded using data loggers. For infrared images, an FLIR A615 IR camera was used. Figure 2 shows the lab experimental setup used in this study.

For these experiments, S54 Rail was used. On the stock rail, thermocouples were installed at three points to record the temperature on the rails. The rail has three main parts, called the head, web, and foot of the rail, and each has its own specific geometry. Moreover, the contact of each part with the switch rail, ground, heater, and clamps is not the same, so it was decided to install thermocouples to observe each area separately. The locations of the thermocouples are shown in Figure 3 with red circles. A control device was designed to control the heater using a temperature controller. This device could read the power consumption by a power meter. Moreover, the temperature data from thermocouples were recorded using the data logger presented in Figure 3.

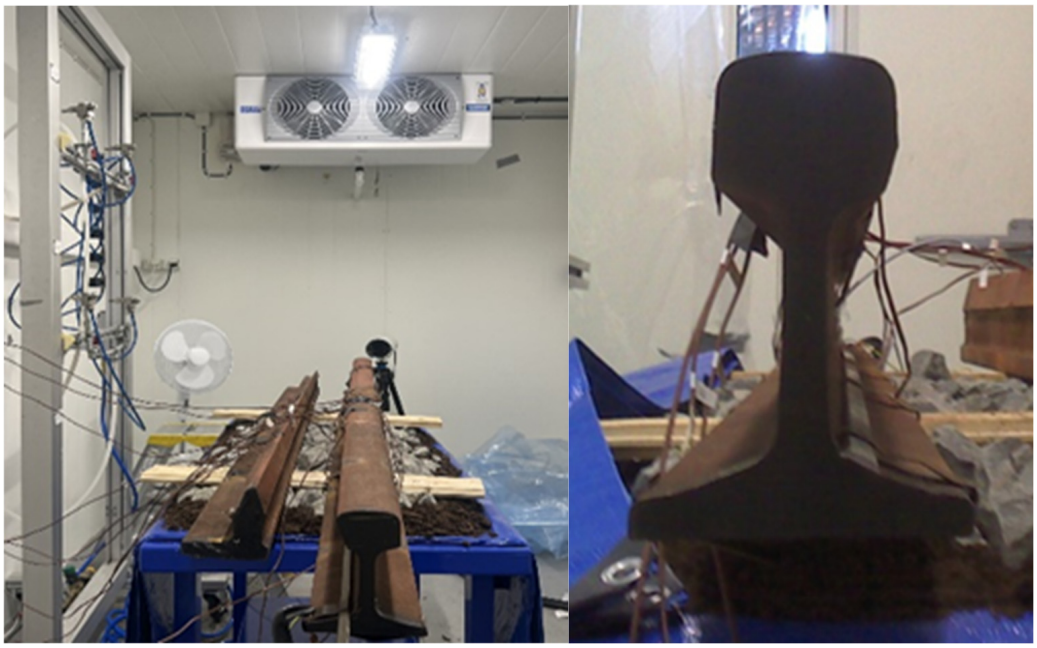

Figure 2. Lab experimental setup.

(**a**) (**b**) (**c**)

Figure 3. (**a**) Location of thermocouples on the rail, (**b**) heat controller, (**c**) data logger.

For the experiments, an infrared-based imaging technique was used to record the dynamic variation in rail surface temperature. An IR camera is a non-contact temperature measurement device that detects the infrared energy emitted, transmitted, or reflected by all materials at temperatures above absolute zero (0° Kelvin) and converts the energy factor into a temperature reading or thermogram [15]. IR images are processed using IR control software V4.59. For the calibration of the IR camera during experiments, firstly, the reflected temperature was examined. To increase the emissivity, the rail surface was covered by a black coating sprayed on the rail cross-section. The reflected temperature, the emissivity of 0.92, and the distance from the object were carefully adjusted for the calibration of IR imaging. Surface temperature measurements from IR cameras were validated with the thermocouples recorded temperatures during the experiments.

For the experiments, heat distribution due to resistive heating along railway switches were observed under different conditions. Experiments were carried out under two different conditions (Table 1). To explain the experimental process, we take scenario 1 as an example, where the air temperature was 268 K (−5 °C). To start the experiment, the room temperature was set to 268 K (−5 °C). It took some time until the rails' temperature reached 268 K (−5 °C) as well (all thermocouples on rails should have shown 268 K), then the control unit automatically switched on the heater. The heating continued until the rail surface temperature reached the target temperature of 278 K (+5 °C). Then, the

heater tried to maintain the rail temperature and automatically switched off. Rail surface temperature and heat distribution were recorded from the start of heating for 20 min. The power consumption of the heater was also recorded during the experiments.

Table 1. Scenarios for lab experiments.

Scenarios	Initial Temperature (K)	Target Temperature (K)
1	268	278
2	253	278

The experimental results gained from the thermocouples and infrared thermography of the rail track were compared with the simulation model. For that purpose, a 2D rail track geometry surrounded by cool air was modeled in MATLAB®2022a and analyzed under heat transfer equations of conduction and convection. Conduction is supposed to take place over metallic rail tracks while natural convection occurs in the air. The rail cross-section model used in the MATLAB simulation is shown in Figure 4.

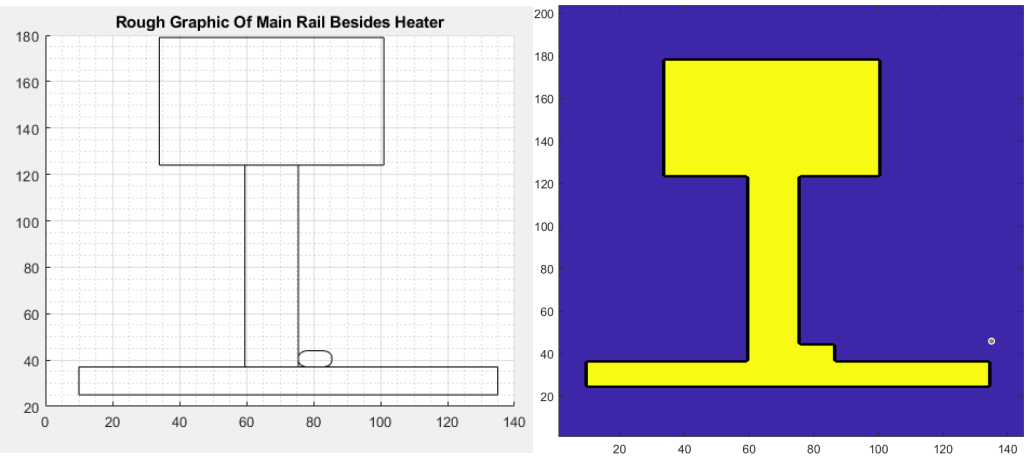

Figure 4. Schematic overview of rail geometry from MATLAB model.

The distribution of conductive heat transfer over a spatial domain with the transition of time can be expressed by a 2nd order differential equation:

$$\frac{\partial T}{\partial t} = \alpha\left(\frac{\partial^2 T}{\partial x^2} + \frac{\partial^2 T}{\partial y^2}\right); \begin{cases} t \geq 0 \\ 0 \leq x \leq L \\ 0 \leq y \leq W \end{cases} \quad (1)$$

where α is the diffusion coefficient of the material, t is the time, and (x,y) are spatial dimensions for length (L) and width (W). The solution for this transient heat equation can be obtained for a finite time if initial conditions (at t = 0) and boundary conditions at (x,y) = (0,0) and (x,y) = (L,W) are known.

In order to solve this partial differential equation, it was discretized using the finite difference method, which meshes the whole surface geometry and transforms continuous time derivatives into difference equations to calculate the solution at all mesh nodes. There are different explicit and implicit integration schemes for finite difference discretization, such as Forward Time-Centered Space (FTCS), Backward Time-Centered Space (BTCS), and Crank–Nicolson. These schemes leverage each other in terms of temporal truncation error, computational effort, and sensitivity towards the selection of time step (Δt) and spatial domain step (Δx, Δy). FTCS was chosen in the case of rail heat transfer as the geometry was simple, and extra computational effort was not required. The transient term for rate of

heat transfer ($\partial T/\partial t$) was replaced by forward difference and spatial terms for heat transfer rate ($\partial T/\partial x$, $\partial T/\partial y$) were replaced with central difference terms, i.e.,:

$$\frac{T_{i,j}^{t+1} - T_{i,j}^{t}}{\Delta t} = \alpha \left(\frac{T_{i+1,j}^{t} - 2T_{i,j}^{t} + T_{i-1,j}^{t}}{(\Delta x)^2} + \frac{T_{i,j+1}^{t} - 2T_{i,j}^{t} + T_{i,j-1}^{t}}{(\Delta y)^2} \right) \quad (2)$$

$$T_{i,j}^{t+1} = T_{i,j}^{t} + \alpha \left(\frac{T_{i+1,j}^{t} - 2T_{i,j}^{t} + T_{i-1,j}^{t}}{(\Delta x)^2} + \frac{T_{i,j+1}^{t} - 2T_{i,j}^{t} + T_{i,j-1}^{t}}{(\Delta y)^2} \right) \Delta t \quad (3)$$

where subscript i, j denote computational points in the spatial domain (x, y plane), (Δx, Δy) formulate the mesh spacing, and Δt is the time step for simulation. The solution for FTCS methodology resembles that of a hyperbolic differential equation, which can become unstable for certain values of α, Δx, Δy, Δt. This instability is defined by a Courant–Friedrichs–Lewy (CFL) condition. As per this criteria, the terms ($\alpha\ \Delta t/(\Delta x^2)$, $\alpha\ \Delta t/(\Delta y^2)$) in the finite difference equations are limited by a maximum value (typically 1) [15]. For this study, the values of α, Δx, Δy, and Δt were chosen so that the Courant number was about 0.1. The values for these parameters, initial/boundary conditions, and some other constants are given in Table 2.

Table 2. Values of parameters for heat transfer study over a rail surface using the finite difference method.

Constant Parameters	
Diffusion Constant (α)	0.1 cm^2s^{-1}
Time Step (Δt)	1 s
Spatial Domain Step (Δx, Δy)	(1 cm, 1 cm)
Initial Conditions	
Metal Sheet Temp.	268 K (−5 °C), 253 K (−20 °C)
Boundary Conditions	
Ambient Air Temp. (all 4 sides)	268 K (−5 °C)
Other Constants	
Heater Temp.	110 K (383 °C)
Heater Turn ON Instant	From t = 5 s

Natural convection was simulated for the air around the rail. For that purpose, the film temperature was calculated as an average of rail surface temperature and ambient air temperature. This film temperature was, in turn, used to calculate viscosity, Prandtl, and Rayleigh numbers, which give the value of convective heat transfer coefficient (h) at varying air temperatures. The rate of convective heat transfer is given by:

$$\frac{dT}{dt} = hA(T_{rs} - T_{amb}) \quad (4)$$

where T_{rs} is the temperature obtained from conduction over the rail surface. Figure 5 explains the analytical model algorithm.

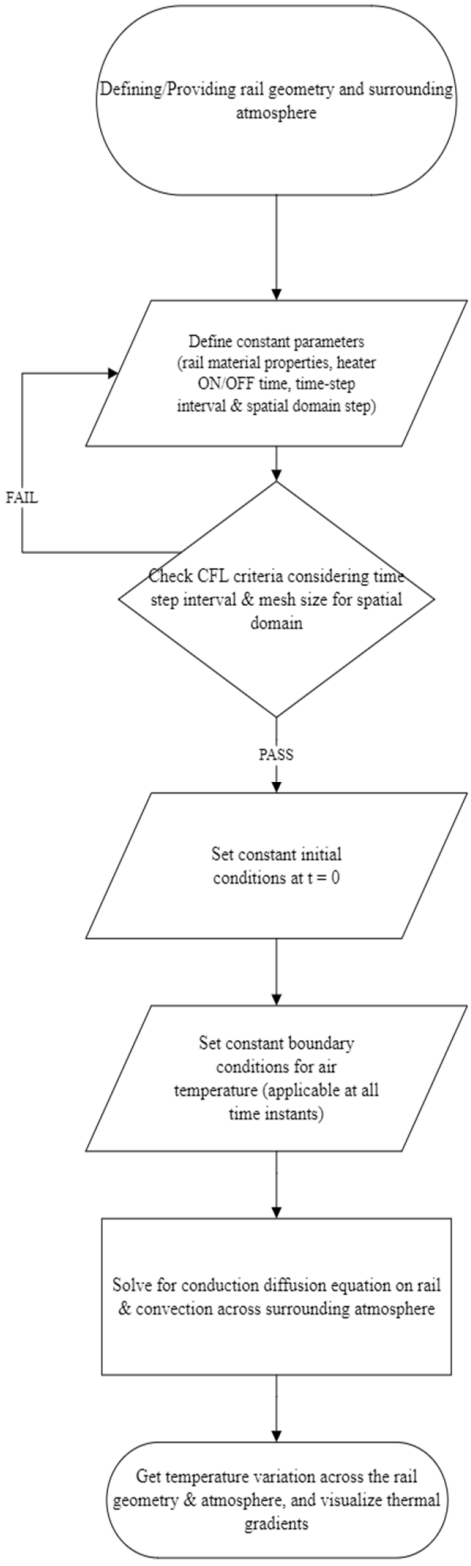

Figure 5. Analytical simulation flowchart.

3. Results

This section provides the results of the laboratory experiment and analytical simulation for heat distribution in two sections.

3.1. Lab Experiments

The lab experiments were carried out under two different sets of operation conditions, specified in Table 1. An infrared camera was used to measure the surface temperature variation, and IR results were compared with the thermocouple temperature values. The aim of this comparison study was to investigate the possibility of using IR cameras in the actual railway field to monitor the temperatures while heaters are operating. Temperatures were recorded using the data logger system. Tables 3 and 4 show the average temperatures in these locations at t = 20 min after the heater was switched on.

Table 3. Average rail temperatures at different locations for atmospheric temperature, T = 268 K (−5 °C).

Scenario	Foot (K)	Web (K)	Head (K)
IR	284.15	277.95	272.95
Thermocouples	284.25	276.85	272.05
Difference (%)	0.03	0.39	0.33

Table 4. Average rail temperatures at different locations for atmospheric temperature, T = 253 K (−20 °C).

Scenario	Foot (K)	Web (K)	Head (K)
IR	272.12	264.84	258.95
Thermocouples	270.13	263.47	256.62
Difference (%)	0.73	0.52	0.90

IR images were further processed and analyzed. For each part of the rail, known as the foot, web, and head of the rail, lines of interest (LOI) were defined to observe the temperature on the line. As the heating process is not symmetrical on the rail, it was not expected to have a smooth temperature distribution on each LOI. Results show that the temperature measurements from IR camera are in good agreement with values from the thermocouples. This highlights the possibility of reliable use of IR cameras for observing the temperatures in actual field conditions of railways.

Figures 6 and 7 show the IR images of temperature distribution along the rail switch cross-section at two different room temperatures. It is observed that the temperature distribution along each section is not constant, and the temperature values fluctuate along each LOI. IR imaging provides more in-depth information along the surface as thermocouples are point devices and can only give the temperature value at one particular point.

According to Figures 6 and 7, most of the heat is transferred to the foot section, especially on the right side where the heater is installed; this means most of the heat generated by the heater is vulnerable to being transferred through the foot into the ballasts under the rail, while the web and head of the rail have a small share of this heat so that the head cannot reach a temperature over 273 K (0 °C). It should be considered that the head has a connection with the switch rail, and it is important for the head to have a higher temperature than 273 K (0 °C).

This pattern is clearly observed in Figure 8 over time; from IR images, the heat transfer over time for a total duration of 20 min was recorded. In this picture, four time sections are shown. The sequence of pictures (1–4) shows how the heat is transferred from the resistive heater to the rail section over time. These pictures also confirm that the heat is mostly transferred to the foot rather than two other sections, which is normal according to the location of the heater. The point is, that this heat transfer cannot be preferable as it is not efficient. While the stock rail needed to be heated in the sections in contact with the moving rail, the heater's energy is mostly consumed to heat up the foot rail and is lost through the foot.

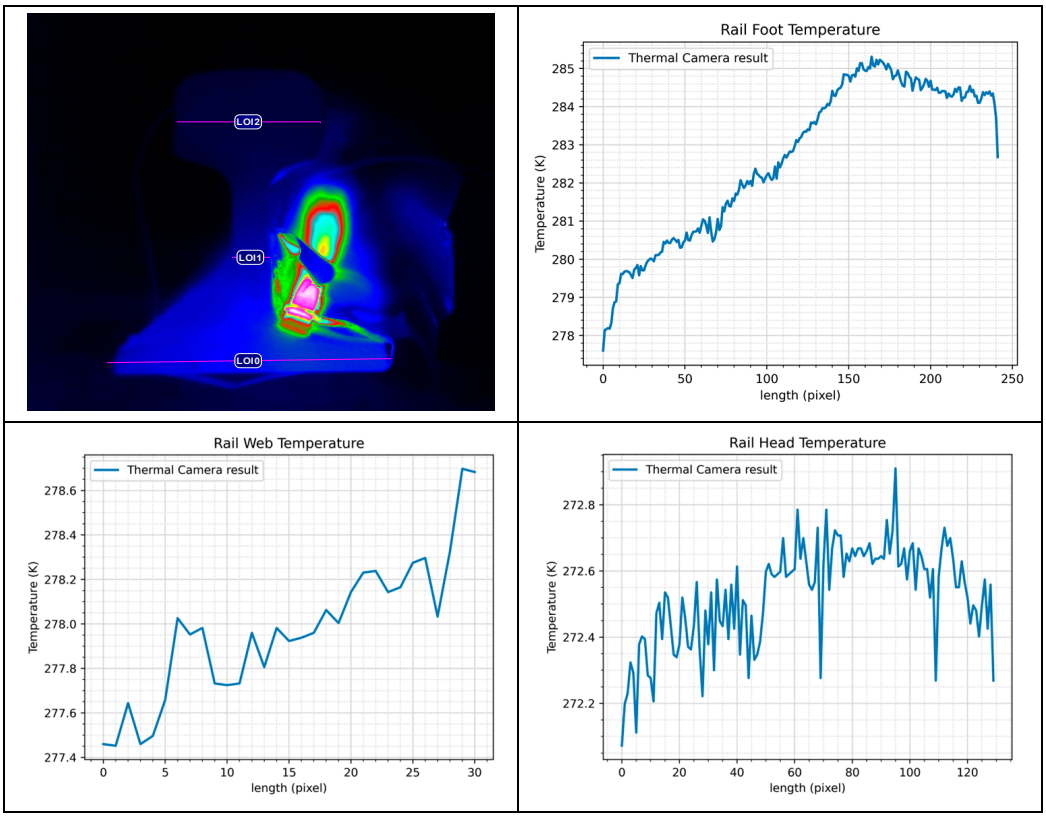

Figure 6. Temperature distribution on LOIs for the temperature of 268.15 K (−5 °C) at t = 20 min.

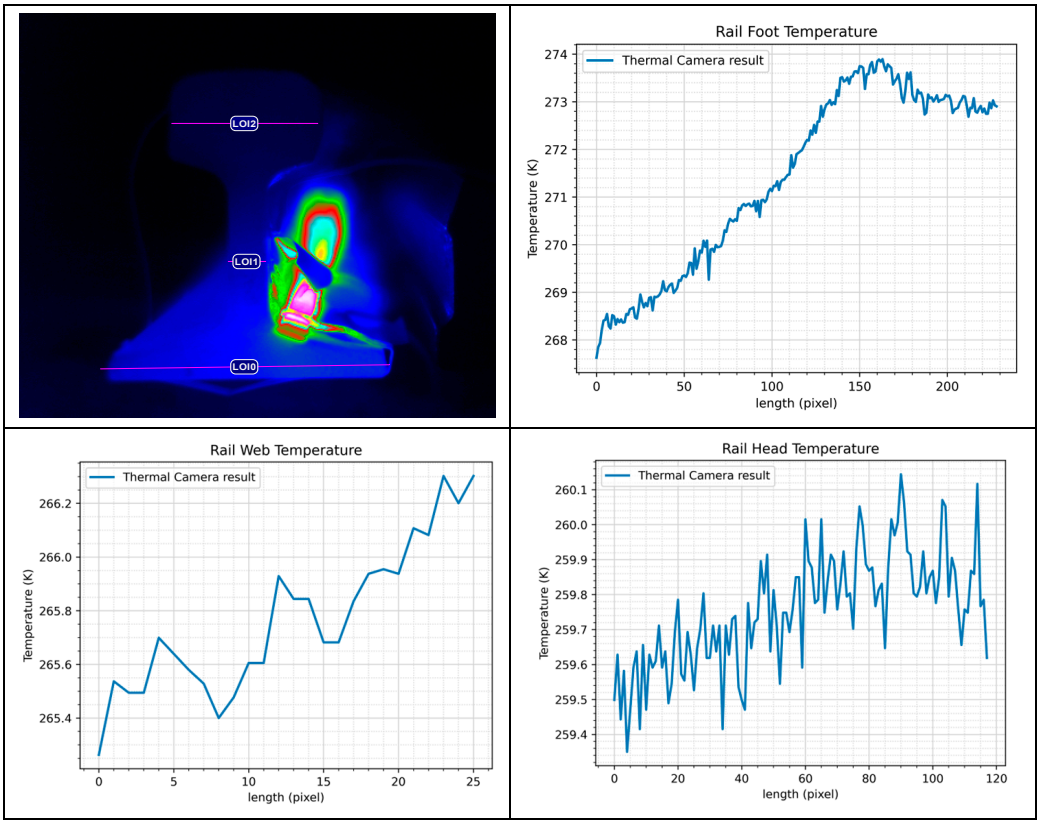

Figure 7. Temperature distribution on LOIs for the temperature of 253.15 K (−20 °C) at t = 20 min.

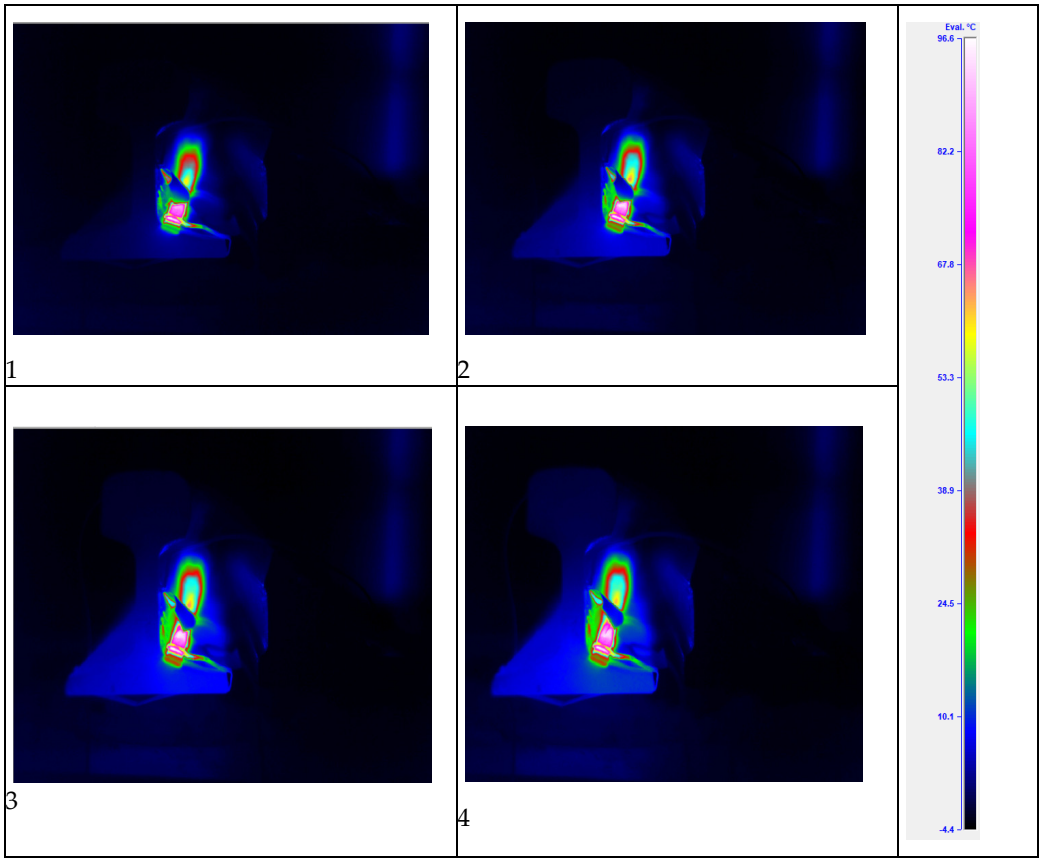

Figure 8. IR images from different steps of heating.

3.2. Analytical Simulations

In this section, the temperatures of different parts of the rail are compared using analytical simulation and experimentation. The approximate locations of thermocouples, which are compared points, are shown in Figure 9. Figures 10 and 11 show the results at the approximate locations of the thermocouples.

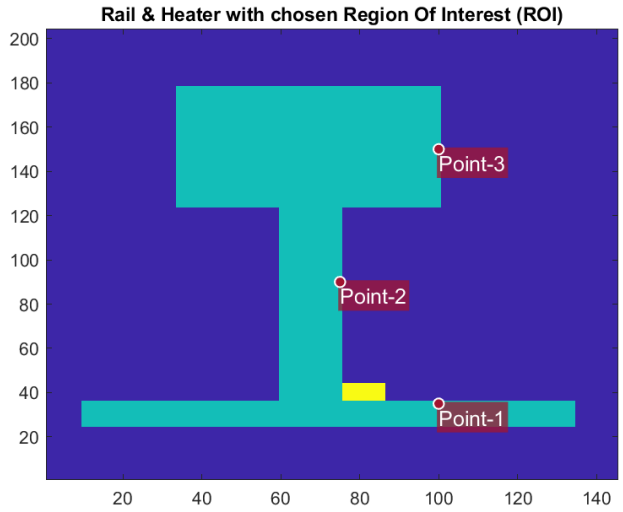

Figure 9. Points of interest.

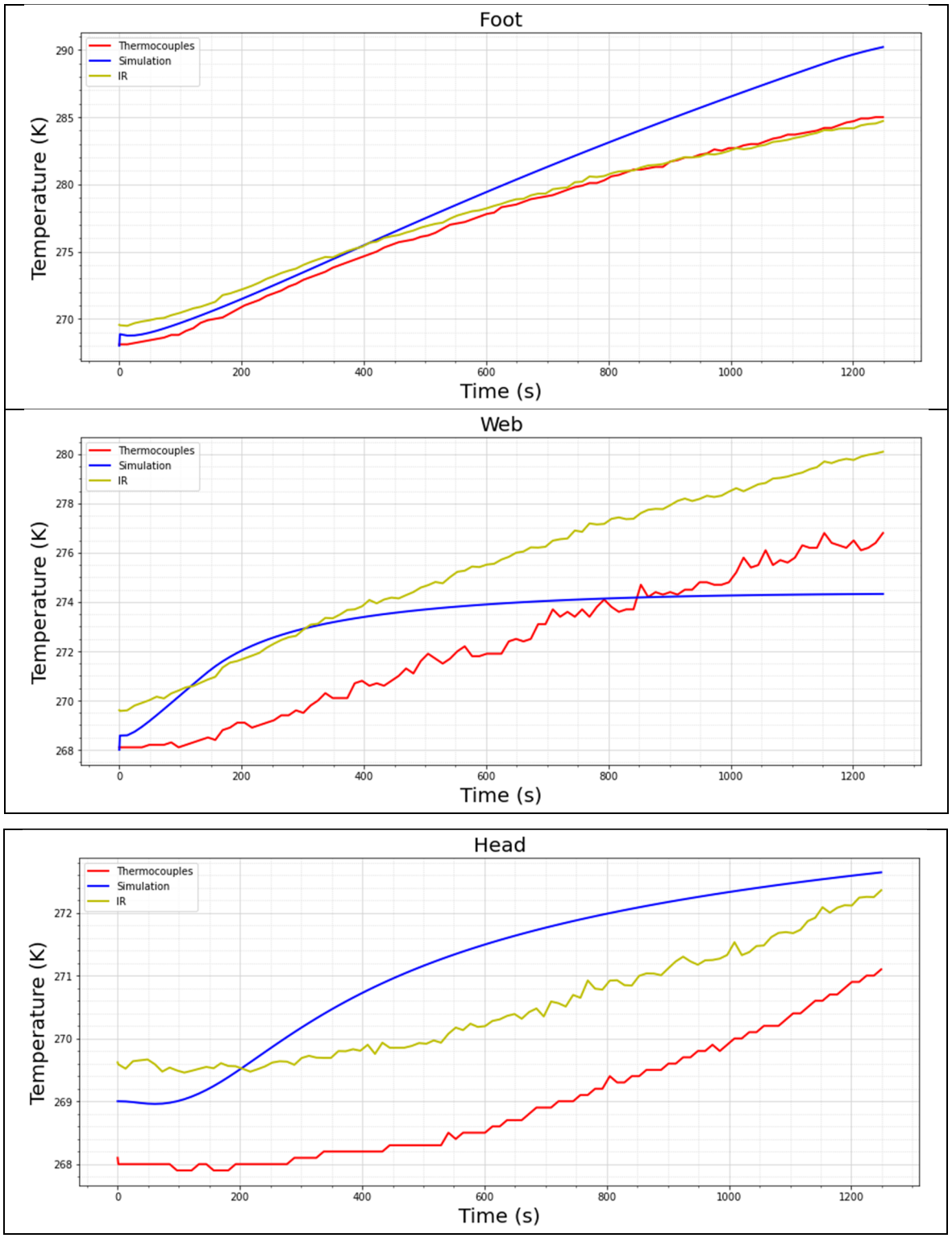

Figure 10. Comparison of measured temperatures using different methods in the ambient temperature of 268 K (−5 °C).

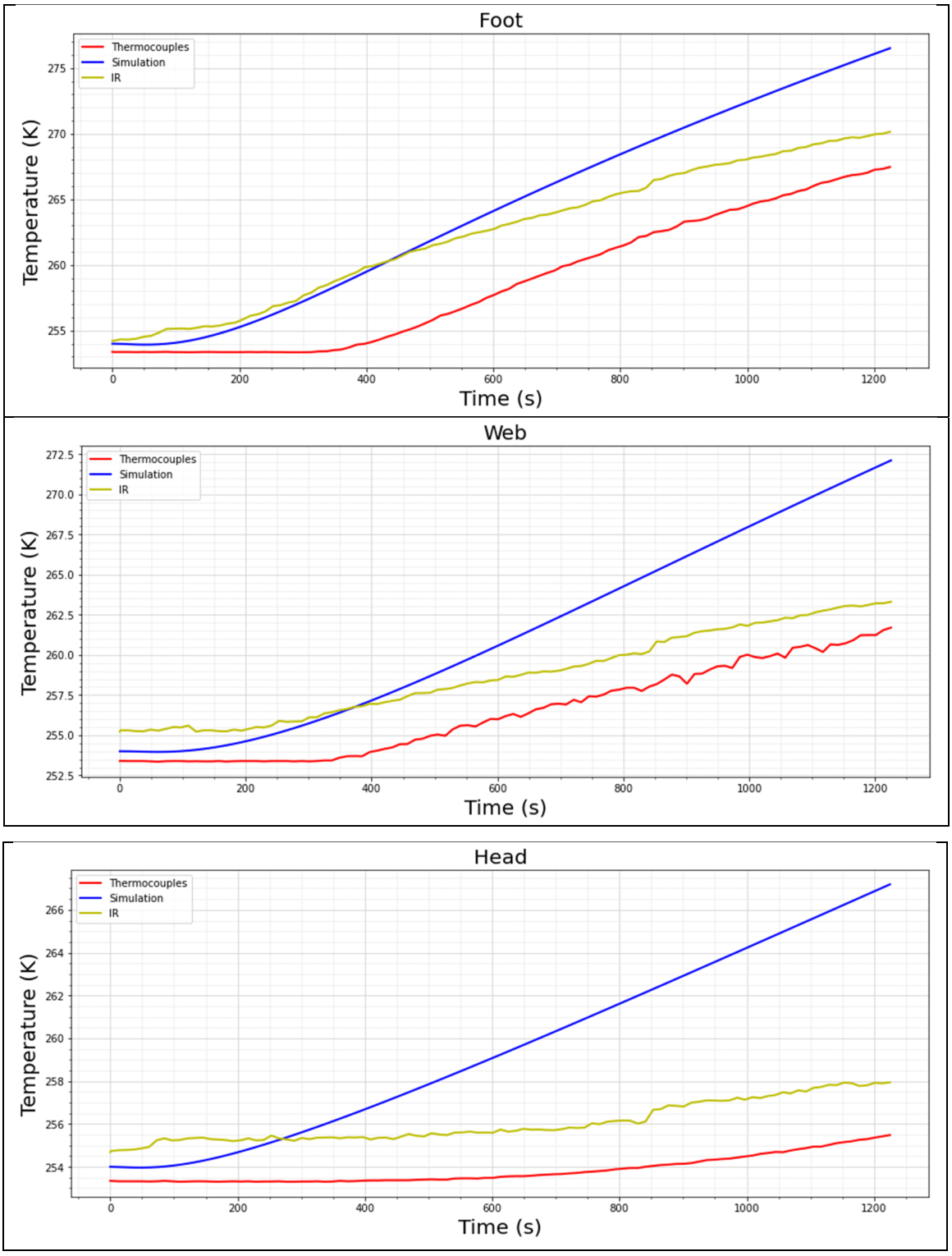

Figure 11. Comparison of measured temperatures using different methods in the ambient temperature of 253 K (−20 °C).

Tables 5 and 6 show the average differences between the simulation and analytical method for all 20 min from the thermocouples, which show small deviations from the values measured by sensors.

Table 5. Percentages of difference from recorded temperatures by thermocouples in the ambient temperature of 268 K (−5 °C).

Scenario	Foot (%)	Web (%)	Head (%)
IR	0.235	1.135	0.563
Analytical	0.857	0.668	0.798

Table 6. Percentages of difference from recorded temperatures by thermocouples in the ambient temperature of 253 K (−20 °C).

Scenario	Foot (%)	Web (%)	Head (%)
IR	1.341	0.853	0.885
Analytical	2.389	2.370	2.724

According to the results, the analytical simulation has a higher temperature deviation in the ambient temperature of 253 K rather than 268 K.

In the following figures, the patterns of temperature increase in all three parts of the rail are presented. The discrepancies in the simulation and experimental results at 268 K and 253 K can be explained precisely in terms of different factors that contributed to such behavior. For the simulation, a cross-sectional rail track geometry was prepared that was close to the actual rail but not exact in shape and surface area (There was a difference of 7.02 cm^2 in surface area from actual rail geometry). This area contributed to the convection rate.

Secondly, within the simulation, the ballasts were not assumed, and hence, heat transfer to them was not accounted for. The heat transfer that took place via the heater installed in the rail foot also resulted in heat loss to the ballast beneath it in experimental results. Thirdly, step heating is assumed in the simulation, i.e., the heater turns ON/OFF instantly without any time delay.

The pattern of curves can be explained with Newton's Law Of Cooling/Heating, which states that the temperature of a body changes at a rate proportional to the difference in temperature between the body and its surroundings. In the scenario where ambient (and initial rail) temperature is 268 K (−5 °C), when the heater starts up, the convection rate is small initially as $\Delta T = T_{rail} - T_{air}$ is small. The rail temperature starts rising gradually and becomes steeper as the body warms up. This leads to a less linear and more curvy temperature profile. In the case of 253 K (−20 °C) ambient air temperature, ΔT is higher, which means that the rate of heat transfer is higher from the very start, and the graph follows a steeper slope.

Figure 12 visualizes temperature distributions within the rail over different time instants when the initial rail temperature was chosen as 269 K with 268 K as ambient temperature. A 1 K difference in temperature is assumed in the initial condition so that a thermal contrast is maintained, and the difference can be noticed. At 5 s, the heater turns ON and remains switched ON for the rest of the simulation. Conduction takes place in the adjacent metallic rail in a semi-circular pattern and extends to heat the foot and web of the rail, as can be seen in images for t = 200 s and t = 1200 s. Near the heater region, the thermal pattern is distinct and more vibrant. Convection in surrounding air is not that apparent in the thermal plot due to its slow rate. As time progresses, the heat transfer due to convection and conduction reduces the temperature differences between the air and metallic rail for the parts away from the heater, and they tend to attain the same temperature as the ambient air. This is apparent in the thermal contour plot at 1200 s, where the left side of the rail foot and upper web try to attain thermal equilibrium with the surrounding air, and the temperature difference there becomes less pronounced. In other words, mathematically, in the conduction equation where $\partial T/\partial t = \alpha \nabla T^2$, the spatial gradient term ∇T tends to become zero there.

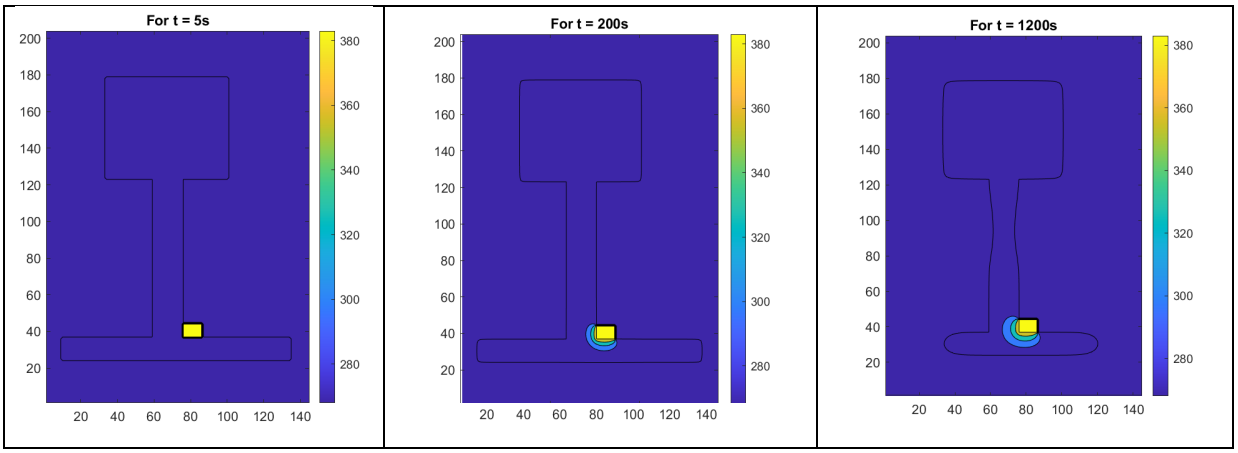

Figure 12. Example of temperature contour (ambient temperature = 268 K).

4. Discussion and Conclusions

This study observed heat flow in a cross-section of a stock rail using an IR camera, thermocouples, and an analytical simulation. The experiment and simulation were performed for continuous heating of the rail for 20 min. Results show that most of the heat generated by the heater is transferred to the rail foot, which provides a condition for heat loss through the ballasts under the rail. Also, the head of the rail, which is an important part according to its connection to the switch rail, experiences a considerable temperature difference with the foot. This temperature difference confirms the mentioned heat loss and supports the idea that the location of the heater is not a suitable one from the heat transfer point of view. This study provides a good base for further optimization of resistive heating operations for ice mitigation along railway switches.

Author Contributions: Conceptualization, A.L. and M.S.V.; methodology, A.L. and M.S.V.; software, A.Y.; validation, A.L. and M.S.V.; writing—original draft preparation, A.L.; writing—review and editing, A.L. and M.S.V.; supervision, M.S.V.; project administration, M.S.V.; funding acquisition, M.S.V. All authors have read and agreed to the published version of the manuscript.

Funding: This research was funded by the Norwegian Research Council, grant number 324156.

Institutional Review Board Statement: Not applicable.

Informed Consent Statement: Not applicable.

Data Availability Statement: If there is interest in the data access through individual requests, the authors can be contacted.

Conflicts of Interest: The authors declare no conflicts of interest.

References

1. Szychta, E.; Szychta, L.; Luft, M.; Kiraga, K. Application of 3D Simulation Methods to the Process of Induction Heating of Rail Turnouts. In *Infrastructure Design, Signalling and Security in Railway*; Xavier, P., Ed.; IntechOpen: Rijeka, Croatia, 2012; p. 12.
2. Fastrax. *Engineered Snow Clearing Products for Rail Applications*; Thermon: Austin, TX, USA, 2021.
3. Omer, R.; Fu, L.P.; Hossain, K.; Muresan, M. *Evaluation and Optimization of Winter Snow and Ice Control Operations for Railway Platforms*; Transportation Planning & Development: Toronto, ON, Canada, 2013.
4. Good Practice Guide-De-Icing Agents for On Station Use. Available online: https://www.raildeliverygroup.com/about-us/publications/acop/241-de-icingagentsforonstationuse/file.html (accessed on 10 August 2023).
5. Ice-Free Switch. Available online: https://www.midwestind.com/rail-lubrication/rail-switch-ice-prevention/ (accessed on 10 August 2023).
6. Żelazny, R.; Jabłoński, P.; Szczegielniak, T. Operation of the Prototype Device for Induction Heating of Railway Turnouts at Various Operating Frequencies. *Energies* **2021**, *14*, 476. [CrossRef]
7. Oh, H.-S.; Park, C.-B.; Lee, S.-H.; Lee, J.-B.; Kim, T.-H.; Lee, H.-W. A study on de-icing for railway turnouts using 250 kHz–200 W-class induction heating system. *AIP Adv.* **2019**, *9*, 125229. [CrossRef]
8. Technology Review of Autonomous Rail Switch Heating System-"Blue Point". *NIBE Element Railway Solutions (US)*, 23 April 2021.

9. Product Catalog, Rails Company. 2007. Available online: www.railsco.com (accessed on 25 March 2023).
10. Wołoszyn, M.; Jakubiuk, K.; Flis, M. Analysis of resistive and inductive heating of railway turnouts. *Przegląd Elektrotechniczny* **2015**, *4*, 54–57. [CrossRef]
11. Szychta, E.; Szychta, L. Comparative Analysis of Effectiveness of Resistance and Induction Turnout Heating. *Energies* **2020**, *13*, 5262. [CrossRef]
12. Flis, M. Energy efficiency analysis of railway turnout heating system with a melting snow model heated by classic and contactless heating method. *Arch. Electr. Eng.* **2019**, *68*, 511–520. [CrossRef]
13. Flis, M. Contactless turnouts' heating for energy consumption optimization. *Arch. Electr. Eng.* **2020**, *69*, 133–145. [CrossRef]
14. Oh, H.; Jeong, G.; Park, C.B.; Jo, I.H.; Kwon, H.; Kim, B.; Han, P.W.; Lee, H.W. A Study on High-Frequency Induction Heating System for Railway Turnout. In Proceedings of the 2019 IEEE 13th International Conference on Power Electronics and Drive Systems (PEDS), Toulouse, France, 9–12 July 2019; pp. 1–4.
15. Courant, R.; Friedrichs, K.; Lewy, H. Über die partiellen Differenzengleichungen der mathematischen Physik. *Math. Ann.* **1928**, *100*, 32–74. [CrossRef]